Received: 7 April 2023 | Revised: 30 May 2023 | Accepted: 2 June 2023 | Published online: 5 June 2023

RESEARCH ARTICLE

Archives of Advanced Engineering Science
2024, Vol. 2(1) 24–29
DOI: 10.47852/bonviewAAES3202944

BON VIEW PUBLISHING

Structural, Elastic, and Mechanical Properties of Cubic Perovskite Materials

Nazia Erum[1,*] and Javed Ahmad[1]

[1]*Institute of Physics, Bahauddin Zakariya University, Pakistan*

Abstract: In this paper, theoretical work has been done on series of cubic perovskites $RbVF_3$, $RbMnF_3$, $RbFeF_3$, $RbCoF_3$, $RbNiF_3$, $RbCuF_3$, and $RbZnF_3$. The main focus is on to compute structural, elastic, and mechanical properties of cubic materials. All subjected computational results are collected by using full-potential linearized augmented plane wave method using the density functional theory. The calculated structural parameters including initial geometry optimization, energy minimization calculations, and total energy values reasonably agree with the previous work. The elastic properties contain C_{11} (for length), C_{12} (for volume), and C_{44} (for shape). These constants are used for calculations of different parameters to discuss mechanical properties. The results show that series of $RbMF_3$ (V, Mn, Fe, Co, Ni, Cu, and Zn) contains metallic bonding and anisotropic behavior. The temperature increases from $RbVF_3$ to $RbZnF_3$. These materials are ductile by nature. However, among all materials, $RbZnF_3$ is the hardest material and also contains the highest melting temperature. Hence, by calculating these useful elasto-mechanical results, they can be applicable in various devices for technological benefits, so the current investigation signifies that these calculations provide a baseline for new researchers to establish further work.

Keywords: perovskite compounds, first-principles study, elastic property, modified Becke–Johnson (mBJ) potential

1. Introduction

The screening of large sets of materials has been possible by machine learning techniques and ab-initio calculations using density functional theory (DFT), though search for new materials for specific applications is attaining huge momentum due to their use in various technologies. Research is conducting on many systems including fluoroperovskites, and investigation results have been reported in recent years through various techniques of DFT (Askar & Shankar, 2016; Attfield et al., 2015; Azulay et al., 2018). The compounds which have general chemical composition of ABF_3 are known as fluoroperovskite compounds. In ABF_3 composition, A and B are cations while (Fluorine) F is an anion. These compounds form an interesting class of materials with mechanically stable crystal structure. These compounds have received much attention in recent years due to their technological importance as scintillation materials, lens material in optical lithography, and radiation dosimeters as well in semiconductor industry. Owing to such broad applications, these compounds are widely examined experimentally and computationally (Ashari-Astani et al., 2019; Adinolfi et al., 2016; Fisher et al., 2004).

These materials are suitable for the fabrication of nanocrystals, nanorods, nanowires, and nanoparticles and are able to be altered to suit various constructions. As a result, technology based on perovskites is estimated to be more cost-effective and appropriate than silicon-based technology (Ablitt et al., 2018; Erum et al., 2021). The cubic material $RbMF_3$ (V, Mn, Fe, Co, Ni, Cu, and Zn) has been studied by keeping in mind their importance. Generally, series $RbMF_3$ (V, Mn, Fe, Co, Ni, Cu, and Zn) crystals crystallize themselves in ideal structure of cubic perovskite that have been experimentally confirmed by Lee et al. (2003) and Burzlaff & Zimmermann (2009). Shafer (1969) investigates unique ferrimagnetic configurations in $RbMgF_3$–$RbCoF_3$ system where Co^{2+} is the only magnetic transition metal ion. Yang et al. (2014), theoretically, explores phenomenon of d-states correlation in potassium-based perovskites $KFeF_3$ and $KCoF_3$. It can be inferred from previous work that $RbCoF_3$ compounds possess advantageous elasto-mechanical aspects.

Elastic properties are highly sensitive to elasto-mechanical parameters, and therefore, accurate calculations of these properties are required in the theoretical studies of the thermoelectric materials for their logical and rational results for practical applications. This paper will dedicate to contribute under cover elasto-mechanical aspects of $RbMF_3$ (V, Mn, Fe, Co, Ni, Cu, and Zn) because as per previous literature review there is inadequate earlier investigation to explore said compounds, so the following compounds require additional research that encourages us to investigate them in detail. In order to accomplish ultimate scientific applications and technological benefits, this paper is organized as follows: Section 1 is devoted to explore few of fundamental aspects of materials as well as their associated applications. Section 2 explains computational method for calculated work, whereas Section 3 represents detailed results plus potential considerations for numerous aspects, and where data available, it is compared with preceding studies. Lastly, conclusion is attained to clarify the upcoming prospective of the research.

2. Computational Methodology

Methods of DFT are often considered be the starting point for determining the electronic structure, even although one uses a

*Corresponding author: Nazia Erum, Institute of Physics, Bahauddin Zakariya University, Pakistan. Email: naziaerum291@gmail.com

Table 1
Bond lengths of $RbMF_3$ (M = V, Fe, Co, and Ni)

$RbVF_3$	Bond length (Å)	$RbMnF_3$	Bond length (Å)	$RbFeF_3$	Bond length (Å)	$RbCoF_3$	Bond length (Å)	$RbNiF_3$	Bond length (Å)	$RbCuF_3$	Bond length (Å)	$RbZnF_3$	Bond length (Å)
Rb – V (Å)	2.4	Rb – Mn (Å)	2.22	Rb – Fe (Å)	2.28	Rb – Co (Å)	2.22	Rb – Ni (Å)	2.22	Rb – Cu (Å)	2.25	Rb – Zn (Å)	2.26
V – F (Å)	2.35	Mn – F (Å)	2.17	Fe – F (Å)	2.23	Co – F (Å)	2.17	Ni – F (Å)	2.17	Cu – F (Å)	2.20	Zn – F (Å)	2.21
Rb – F (Å)	2.99	Rb – F (Å)	2.99	Rb – F (Å)	2.99	Rb – F (Å)	2.99	Rb – F (Å)	2.99	Rb – F (Å)	2.99	Rb – F (Å)	2.99

function that is commonly found in artistic information, which is appropriate – electron gas bonds, calculation of rare or more complex gases more complex level methods. In this paper, DFT is used to evaluate structural, elastic, and mechanical properties of rubidium-based cubic perovskites material $RbMF_3$ where M = V, Mn, Fe, Co, Ni, Cu, and Zn. The entire calculations were executed by using Wien2k code self-consistent full-potential linearized augmented plane wave method within DFT framework to solve Kohn–Sham equations (Blonco et al., 2004; Erum et al., 2022; Yang et al., 2014; Tran & Blaha, 2009). The exchange and correlation potentials employed in DFT were calculated using local density approximation and generalized gradient approximation (GGA) method (Erum et al., 2022; Tran & Blaha, 2009).

The volume optimization was achieved by studying the total energy in terms of symmetry elements. In the irreducible wedge of the Brillouin zone, the total energy optimization has been done with mesh containing 10 × 10 × 10 k-points. In WIEN2K package, valence electron treatments have been done semirelativistically, although core electrons are treated fully relativistically. However, for convergence in basis size, a cut-off value of $RMTK_{max} = 8.0$ is used. The self-consistent field convergence was reduced up to 0.00001 Ry. The value of maximum angular momentum lmax was adjusted at 7. Furthermore, energy and charge convergence standards were set to 0.0001 and 0.001 Ry individually (Francisco et al., 1998; Ayad et al., 2020).

3. Results and Discussions

This section is dedicated to cover detailed structural, elastic, and mechanical parameters of $RbMF_3$, where M = V, Mn, Fe, Co, Ni, Cu, and Zn are perovskite compounds. Further, all current investigation is compared with the previously available data of the related series of perovskite compounds.

3.1. Structural properties

To determine the ground state parameters of the fluoroperovskite $RbMF_3$ where (M = V, Mn, Fe, Co, Ni, Cu, and Zn) different volumes around the equilibrium cell volume are calculated using total energy values. Calculated equilibrium lattice parameters are presented in Table 1. It could be inferred from Table 1 that DFT as well as analytical calculations of lattice constants shows few deviations between 4% and 5%. There are many reasons for these deviations. The empirical relations to calculate the VJ method (lattice constant) depend on the average of ionic radii. On the other hand, observed relations to calculate the above method depend on each electron while error can be due to constants K (2.45) and S (0.09) that contained in this relationship (Reuss & Angew, 1929). So, it means we can conclude that empirical relation given by VJ method can adjust improvement to get accurate values of lattice constants. The bond length parameter is important to calculate the bonding nature. This is the other aspects to calculate or know the structural properties of fluoroperovskites. The length of bond reduces as we go from vanadium to zinc because size reduces from vanadium to zinc.

3.2. Elastic properties

Elastic aspects of a material clarify many mechanical parameters which are influence of crystal to external forces like, strength, mechanical stability, acoustic phonon frequencies, ductility, or brittleness Debye temperature. The explanation of the mechanical behavior of crystalline solids is given by elastic

properties. Using the elastic properties, the phenomena of solid state can be discussed or explained, for example, equation of state and intra-traditional mechanical and cubic stability condition P = 0 GPa which can be described by the relation: C_{11}-$C_{12} > 0$, $C_{11} > 0$, $C_{44} > 0$, $C_{11} + 2C_{12} > 0$ (mechanical stability condition), and $C_{12} < B < C_{11}$ (cubic stability condition). In general, these relationships help us to know about mechanical stability and cubic stability, respectively. Table 2 shows that elasticity in length C_{11} is the highest for zinc-based perovskites $RbZnF_3$, but it is the lowest for $RbVF_3$ because size reduces from vanadium to zinc and I-e radius increases from vanadium to zinc due to increase in mass number (A) as per periodic table. The elasticity in volume is explained by C_{12}. The present calculations show that $RbMF_3$ has a trend of increase of C_{12} from vanadium to zinc. Shape elasticity could explain by well using elastic constant C_{44}. Thus, the current result shows $RbMF_3$ has a trend of increase of C_{44} from vanadium to zinc as shown in Table 3 (Jenkins & Khanna, 2005).

3.3. Mechanical properties

The elastic constants have been utilized to calculate important mechanical properties. For example, thermos-elastic stress and strain (internal) are very important for mechanical properties in case of industry. The GGA approximations are used to calculate mechanical properties, as shown in Tables 2 and 4, respectively. The Voigt Reuss Hill method is used to describe bulk modulus and shear modulus. The shear modulus G is used to measure the resistance to reversible deformation by using the following relation (Pettifor, 1992):

$$G_V = 1/5(C_{11} - C_{12} + 3C_{44}) \quad (1)$$

$$G_H = (G_V + G_R)/2 \quad (2)$$

The bulk modulus B is calculated by using the following relation:

$$B = 1/3(C_{11} + 2C_{12}) \quad (3)$$

This table shows that $RbZnF_3$ contains the highest values and has smallest value $RbVF_3$ of both bulk and shear modulus. By calculations, $RbZnF_3$ is the hardest and remaining compounds are less hard as compared to it.

The linear strain of materials is described by Young's modulus "Y" with its relation. There is also another important factor called Pugh's index of ductility or B/G. B/G < 1.75 and B/G > 1.75 are used to describe brittle and ductile behavior of materials, respectively. The $RbMF_3$ series of compounds shows ductile behavior because this series obeys condition for Pugh's index of ductility.

Table 2
Calculated values of bulk modulus B_0, Voigt's shear modulus G_V, Reuss shear modulus G_R, Hill's shear modulus G_H, Young's modulus Y, and Pugh's index of ductility B_o/G_H

Sr. no.	Parameters	$RbVF_3$	$RbMnF_3$	$RbFeF_3$	$RbCoF_3$	$RbNiF_3$	$RbCuF_3$	$RbZnF_3$
1	B_o(GPa)	61.1	67.37	69.36	74.2	90.83	98.26	106.49
2	Gv(GPa)	25.44	26.47	28.103	29.04	33.62	38.20	41.59
3	G_R(GPa)	24.13	25.58	27.49	28.90	33.20	38.10	41.58
4	G_H(GPa)	24.785	26.02	27.79	28.97	33.41	38.15	41.58
5	Y(GPa)	65.5	69.15	73.54	76.90	89.28	101.33	110.37
6	B_o/G_H (GPa)	2.46	2.589	2.495	2.56	2.71	2.575	2.561

Table 3
Calculated values of elastic constants C_{11}, C_{12}, C_{44}, for $RbMF_3$ (M = V, Fe, Co, Mn, Cu, Zn, and Ni) compounds

Sr. no.	Parameters	$RbVF_3$	$RbMnF_3$	$RbFeF_3$	$RbCoF_3$	$RbNiF_3$	$RbCuF_3$	$RbZnF_3$
1	C_{11} (GPA)	104.9	110.91	113.85	116.2	141.9	152.30	162.67
2	C_{12} (GPA)	39.2	45.60	47.126	53.2	65.3	71.24	78.40
3	C_{44} (GPA)	20.2	22.36	24.597	27.4	30.5	36.65	41.23

Table 4
Calculated values of shear constant (C'), Cauchy's pressure (C''), Poisson's ratio, (ν), anisotropy constant (A), Kleinman's parameter (ξ), Lame's coefficients (λ and μ), and melting temperature (T_m)

Sr. no.	Parameters	$RbVF_3$	$RbMnF_3$	$RbFeF_3$	$RbCoF_3$	$RbNiF_3$	$RbCuF_3$	$RbZnF_3$
1	C'	32.85	32.65	33.36	31.5	388.3	40.53	42.14
2	C''	18.7	23.24	22.529	25.8	34.8	34.59	37.17
3	ν (GPa)	0.32	0.3285	0.32	0.327	0.336	0.3280	0.3270
4	A (GPa)	0.92	0.68	1.10	1.30	1.19	0.90	0.97
5	ξ(GPa)	0.64	0.69	0.70	0.766	0.77	0.78	0.80
6	Λ	44.46	49.97	49.52	57.049	68.45	72.76	78.61
7	M	43.26	26.02	27.85	51.023	59.63	38.15	41.58
8	Tm(K)	1730.23	1788.54	1807.05	1852.06	2006.72	2075.81	2152.35

3.4. Calculations of Cauchy's pressure and shear constant

The angular behavior can be described by Cauchy's pressure. Its relation is (Pugh, 1954)

$$C'' = C_{12} - C_{44} \quad (4)$$

The compounds with negative values of Cauchy's pressure have high angular behavior in bonding. But compounds with positive values of Cauchy's pressure have metallic bonding nature. The condition of B/G >1.75 and $C'' > 0$ shows that $RbMF_3$ materials are ductile by nature. Its relation is

$$C'' = 1/2(C_{11} - C_{12}) \quad (5)$$

It can be evaluated that Table 5 shows that $RbMF_3$ contains high values for shear constant. So, they retain dominant metallic bonding.

3.5. Calculations of Poisson's ratio and elastic anisotropy

The finding revealed that Poisson's ratio expresses the ratio of compression to relative expansion. According to the relation (Majid et al., 2010):

$$v = (3B_\circ - 2GH)/2(3B_\circ + GH) \quad (6)$$

According to Gu and his colleagues, the upper and lower limits are 0.25 and 0.5. On the other hand, Haines with his research helpers stated that it is less than 0.1 for ionic materials, resisting greater to ionic behavior and lesser to covalent behavior. Thus, it is resulted from many mechanical properties that $RbMF_3$ compounds contain superior to covalent behavior. The elastic anisotropy factor (A) has vital role in manufacturing process. Its relation is

$$A = 2C_{44}/(C_{11} - C_{12}) \quad (7)$$

The crystals which are completely isotropic, they have A=1 but value is deviated from A=1 if micro-cracks are found in crystals. Then, degree of deviation gives elastic anisotropy. However, A<1 for $RbMF_3$ shows the anisotropic behavior of these perovskite compounds. The addition of cations with smaller atomic size leads to reduce in anisotropy.

3.6. Calculations of melting temperature and Kleinman's parameter

This work is sponsored the temperature above which solid state is changed to liquid state is called melting temperature (T_m). This property of $RbMF_3$ is calculated now as (Erum & Iqbal., 2017):

$$T_m = 607 + 9.3B_\circ + 555 \quad (8)$$

Figure 1 shows that the melting temperature (T_m) increases with the increase of elastic constant in length (C_{11}). It is shown from graph that $RbVF_3$ has low melting temperature due to its smaller elastic constant in length. Graph shows that melting temperature has smaller difference from $RbVF_3$ to $RbCoF_3$. After $RbCoF_3$, melting temperature has more difference for compounds. Graph shows that melting temperature increases from $RbVF_3$ to $RbZnF_3$ due to increase in stability.

The GGA calculations of melting temperature are actually dependent on behavior of compounds. This temperature changes as compounds of type $RbMF_3$ change. The temperature increases from $RbVF_3$ to $RbZnF_3$ because bond length decreases and modulus increases from $RbVF_3$ to $RbZnF_3$. Figure 2 shows that the melting temperature (T_m) increases with the increase of bulk modulus (B_o). It is shown from figure that $RbVF_3$ has low melting temperature due to its smaller bulk modulus (B_o). It can be seen that melting temperature has smaller difference from $RbVF_3$ to $RbCoF_3$. After $RbCoF_3$, melting temperature has more difference for compounds. Graph shows that melting temperature increases from $RbVF_3$ to $RbZnF_3$ due to increase in stability. Figure 3 shows that the melting temperature (T_m) increases with the increase of Young's modulus (Y). It is shown from figure that $RbVF_3$ has low melting temperature due to its smaller elastic constant in length which shows that melting temperature has

Figure 1
The melting temperature (T_m) vs elastic constant in length (C_{11})

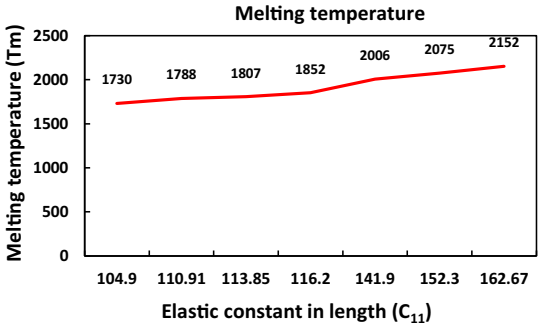

Figure 2
Melting temperature (Tm) vs increase of bulk modulus

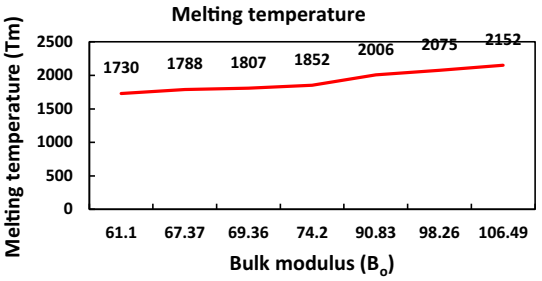

Figure 3
Melting temperature (T_m) vs increases with the increase of Young's modulus (Y)

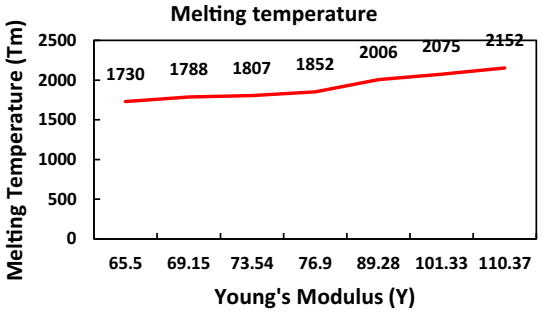

smaller difference from $RbVF_3$ to $RbCoF_3$. However, melting temperature increases from $RbVF_3$ to $RbZnF_3$ due to increase in stability. Figure 4 shows anisotropic constant (A) deals with the deviation of bonding. If A = 1, the compound is called isotropic. However, if A is not equal to 1, then it is called anisotropic. Degree of deviancy of A from 1 decides elastic anisotropic constant. The graph in Figure 4 shows that $RbFeF_3$ has values of A more near to 1. The anisotropic behavior decreases from left to right. $RbMnF_3$ > $RbNiF_3$ > $RbCuF_3$ > $RbVF_3$ > $RbCoF_3$ = $RbZnF_3$ > $RbFeF_3$. $RbZnF_3$ and $RbCoF_3$ have same degree of deviation from 1 that has same behavior for anisotropy.

Figure 4
Anisotropic constant (A) vs elastic constant in length (C_{11})

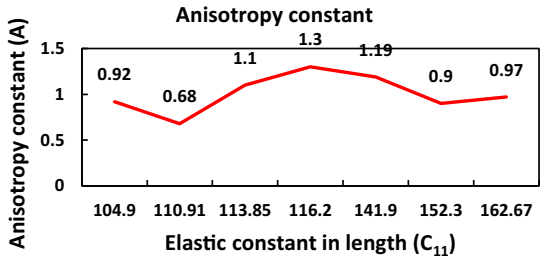

One of the other parameters (ξ) given by Kleinman quantitatively describes behavior of materials about bonding, that is, deviation in bonding. If bond deviation or stretching is minimum, then Kleinman's parameters will be ξ = 1, and if materials have minute values of bond bending or stretching or deviation, then ξ = 0.

The relation is as follows:

$$\xi = (C_{11} + 8C_{12})/(7C_{11} - 2C_{12}) \tag{9}$$

Figure 5 reveals Kleinman's parameter Vs increases then melting temperature also increases. Kleinman's parameter is maximum for $RbZnF_3$ and minimum for $RbVF_3$. Melting temperature more increases for $RbNiF_3$, $RbCuF_3$ and $RbZnF_3$. Kleinman's parameter is highest for $RbZnF_3$ and lowest for $RbVF_3$.

Figure 5
Kleinman's parameter vs melting temperature

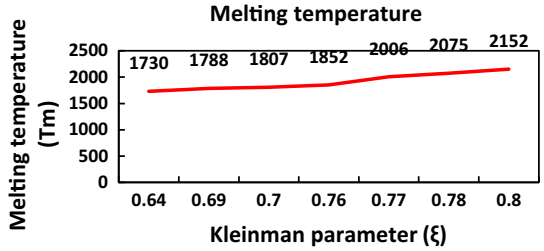

3.7. Calculations of melting temperature and Kleinman's parameter

The authors by taking two constants named as λ and μ Lame's constants then we can study stress to strain. The expression of these constants is in the form:

$$\lambda = y\upsilon/(1+\upsilon)(1-2\upsilon) \tag{10}$$

$$\mu = y/2(1+\upsilon) \tag{11}$$

These relations show that λ and μ are related to Y. Our calculated values do not obey condition $\lambda = C_{12}$ and $\mu = C'$ for isotropic compounds. So, $RbMF_3$ is series of anisotropic materials which is result as that of calculation. Hence, the increase in anisotropic behavior is as $RbVF_3$ to $RbNiF_3$.

4. Conclusion

The nature of bonding changes from material to material. So, theoretical simulation is used as computations of approximations to the bonding. The work is done in this paper using theoretical simulation. The main focus is on to compute structural, elastic, and mechanical properties of cubic perovskite materials. The cubic materials are $RbVF_3$, $RbMnF_3$, $RbFeF_3$, $RbCoF_3$, $RbNiF_3$, $RbCuF_3$, and $RbZnF_3$. The calculation for these materials is done using DFT by using WIEN2K method. The melting temperature (T_m) increases with the increase of elastic constant in length (C_{11}). $RbVF_3$ has low melting temperature due to its smaller elastic constant in length. The melting temperature has smaller difference from $RbVF_3$ to $RbCoF_3$. After $RbNiF_3$, $RbCuF_3$, and $RbZnF_3$, melting temperature has more difference among compounds. The melting temperature (Tm) increases with the increase of bulk modulus (Bo). $RbVF_3$ has low melting temperature due to its smaller bulk modulus (B_o). The melting temperature has smaller difference from $RbVF_3$ to $RbCoF_3$. The melting temperature (T_m) increases with the increase of Young's modulus (Y). $RbVF_3$ has low melting temperature due to its smaller elastic constant in length. The melting temperature has smaller difference from $RbVF_3$ to $RbCoF_3$. After $RbCoF_3$, melting temperature has more difference for compounds. $RbFeF_3$ has values of A more near to 1. So, it is less isotropic. $RbMnF_3$ has more deviation from 1. So, it means $RbMnF_3$ is a more anisotropic compound. The degree of deviation is due to cracking problem in structure. As Kleinman's parameter increases, the melting temperature also increases. Kleinman's parameter is maximum for $RbZnF_3$ and minimum for $RbVF_3$. Melting temperature more increases for $RbNiF_3$, $RbCuF_3$, and $RbZnF_3$ while Kleinman's parameter is highest for $RbZnF_3$ and lowest for $RbVF_3$.

Conflicts of Interest

The authors declare that they have no conflicts of interest to this work.

Data Availability Statement

Data sharing is not applicable to this article as no new data were created or analyzed in this study.

References

Ablitt, C., Mostofi, A. A., Bristowe, N. C., & Senn, M. S. (2018). Control of uniaxial negative thermal expansion in layered perovskites by tuning layer thickness. *Frontiers in Chemistry*, *6*, 455.

Adinolfi, V., Yuan, M., Comin, R., Thibau, E. S., Shi, D., Saidaminov, M. I., . . . , & Sargent, E. H. (2016). The in-gap electronic state spectrum of methylammonium lead iodide single-crystal perovskites. *Advanced Materials*, *28*(17), 3406–3410.

Ashari-Astani, N., Jahanbakhshi, F., Mladenovic, M., Alanazi, A. Q. M., Ahmadabadi, I., Ejtehadi, M. R., . . . , & Rothlisberger, U. (2019).

Ruddlesden-Popper phases of methylammonium-based two-dimensional perovskites with 5-ammonium valeric acid AVA2MA n-1Pb nI3 n+1 with n = 1, 2, and 3. *Journal of Physical Chemistry Letters*, *10*(13), 3543–3549.

Askar, A. M., & Shankar, K. (2016). Exciton binding energy in organic-inorganic tri-halide perovskites. *Journal of Nanoscience and Nanotechnology*, *16*(6), 5890–5901.

Attfield, J. P., Lightfoot, P., & Morris, R. E. (2015). Perovskites. *Dalton Transactions*, *44*(23), 10541–10542.

Ayad, M., Belkharroubi, F., Boufadi, F. Z., Khorsi, M., Zoubir, M. K., Ameri, M., . . . , & Bensaid, D. (2020). First-principles calculations to investigate magnetic and thermodynamic properties of new multifunctional full-Heusler alloy Co2TaGa. *Indian Journal of Physics*, *94*, 767–777.

Azulay, D., Levine, I., Gupta, S., Barak-Kulbak, E., Bera, A., San, G., . . . , & Balberg, I. (2018). On the influence of multiple cations on the in-gap states and phototransport properties of iodide-based halide perovskites. *Physical Chemistry Chemical Physics*, *20*(37), 24444–24452.

Blonco, M. A., Frencisco, E., & Luana, V. (2004). GIBBS: isothermal-isobaric thermodynamics of solids from energy curves using a quasi-harmonic Debye model. *Computer Physics Communications*, *158*(1), 57–72.

Burzlaff, H., & Zimmermann, H. (2009). On symmetry classes of crystal structures. *Acta Crystallographica Section A: Foundations and Advances, 65*, 456–465.

Erum, N., Iqbal, M. A., & Ashraf, F. (2022). Effect of hydrostatic pressure on structural and opto-electronic properties for Barium based Oxide perovskite, *Physica Scripta*, *97*(4), 045802.

Erum, N., Iqbal, M. A., & Bashir, I. (2021). A DFT study of structural, electronic and optical properties of pristine and intrinsic vacancy defects containing barium zarconate (BaZrO3) using mBJ potential. *Physica Scripta, 96*(2), 025807.

Erum, N., & Iqbal, M. A. (2017). Study of pressure variation effect on structural, opto-electronic, elastic, mechanical, and thermodynamic properties of SrLiF3. *Physica B: Condensed Matter*, *525*, 60–69.

Fisher, B., Chashka, K. B., Patlagan, L., & Reisner, G. M. (2004). Berthelot type conductivity of porous: Sr2CrReO6 examination of an old empirical relation, *Physical Review B*, *70*(20), 205109.

Francisco, E., Recio, J. M., Blonco, M. A., & Pendas, A. M. (1998). Quantum-mechanical study of thermodynamic and bonding properties of MgF2. *The Journal of Physical Chemistry A*, *102*(9), 1595–1601.

Jenkins, C., & Khanna, S. (2005). *Mechanics of Materials: A Modern Integration of Mechanics and Materials in Structural Design*. USA: Academic Press.

Lee, J., Shin, H., Chung, H., Zhang, Q., & Saito, F. (2003). Mechanochemical syntheses of perovskite KMIIF3 with cubic structure (MII = Mg, Ca, Mn, Fe, Co, Ni, and Zn). *Materials Transactions*, *44*(7), 1457–1460.

Majid, A., Khan, A., Javed, S. G., & Majid, A. M. (2010). Lattice constant prediction of cubic and monoclinic perovskites using neural networks and support vector regression. *Computational Materials Science, 50*(2), 363–372.

Pettifor, D. G. (1992). Theoretical predictions of structure and related properties of intermetallics. *Materials Science and Technology*, *8*(4), 345–349.

Pugh, S. F. (1954). Relations between the elastic moduli and the plastic properties of polycrystalline pure metals. *The London, Edinburgh, and Dublin Philosophical Magazine and Journal of Science*, *45*(367), 823–843.

Reuss, A., & Angew, Z. (1929). Berechnung der Flieggrenze von Mischkristallen auf Grund der Plastizitätsbedinung für Einkristalle (in German). *Journal of Applied Mathematics and Mechanics*, *9*(1), 49–58.

Shafer, M. W. (1969). Magnetic and optical properties of ferrimagnets in the RbMgF3–RbCoF3 system. *Journal of Applied Physics*, *40*(3), 1601.

Tran, F., & Blaha, P. (2009). Accurate band gaps of semiconductors and insulators with a semilocal exchange-correlation potential. *Physical Review Letters*, *102*(22), 226401.

Yang, L., Dacek, S., & Ceder, G. (2014). Proposed definition of crystal substructure and substructural similarity. *Physical Review B, 90*(5), 054102.

How to Cite: Erum, N. & Ahmad, J. (2024). Structural, Elastic, and Mechanical Properties of Cubic Perovskite Materials. *Archives of Advanced Engineering Science,* 2(1), 24–29, https://doi.org/10.47852/bonviewAAES3202944